CHARACTERIZATION OF SAR MODE ALTIMETRY OVER INLAND WATER

Pierre Fabry[(1)] and Nicolas Bercher[(1)]

[(1)]ALONG-TRACK S.A.S., 43B rue de Bertheaume, 29217, Plougonvelin, France

pfabry@along-track.com

ABSTRACT

Radar altimetry over the inland water domain is a difficult topic that still requires a lot of human expertise as well as manual editing and verifications. This is mainly due to the fact that inland water scenes are highly variable, both in space and time, which leads to a much broader range of radar signatures than in oceanography. The remark is particularly true for LRM altimetry and remains valid in many cases in SAR mode (SARM). In preparation for the operational Sentinel-3 mission and to better benefit from the improved SARM along-track resolution it is required to:

1. better characterize the SARM Individual Echoes, Multi-Look Stacks, 20Hz waveforms as well as the Range Integrated Power (RIP) over the inland water domain,
2. step toward processing schemes that account for the actual content of the illuminated scene.

In this work, we introduce an automated technique to assess the water fraction within the Beam-limited Doppler footprint through its intersection area of with a water mask. This framework opens up new ways toward the automated characterization and processing of altimetry data based on regularly updated water masks.

1. CONTEXT

The main reason why Space Hydrology is still not operational at global scale is the variety of inland water scenes and scenarios which cannot properly be taken into account via a single and fixed processing chain. The complexity coming from the spatial diversity is emphasized by the strong temporal variability related to seasonal trends, extreme events and human action. Rivers and lakes' bathymetry and contours do change over time. Sand banks and islands appear, disappear or change from shape and location. In addition, the radar backscatter properties of water depend on wind conditions, surface current and trophic phenomenons. Not to forget the specific cases of mountain lakes and the vicinity of cities or other strong radar reflectors. Several of these aspects may be mixed together at small spatial scale (few km).

Figure 1 illustrates the complexity of LRM radar altimeter waveforms (Jason-2) on a “standard” case in the Amazon (rio Madeira) involving water and forest surfaces. Figure 2 confirms that CryoSat-2 SAR mode also exhibit portions of hyperboles due to dominant across-track off-nadir water areas (Amazon).

As a matter of fact it has already been shown that SARM radar echoes are sensitive to strong off nadir reflectors. This is depicted by the “loss” of the ground tracks pattern in Figure 3 that plots CryoSat-2 SARIn products over the Amazon [Bercher et al., 2014a].

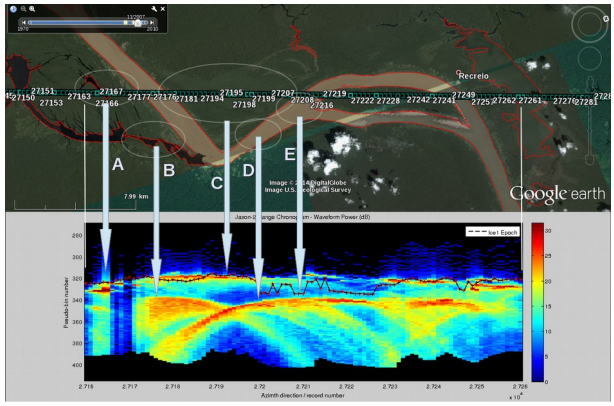

Figure 1. Jason-2 waveforms Range-Chronogram (S-GDR products) over the Madeira river (Brazil). The ICE1 retracker outputs are superimposed (red crosses linked by a black line). ICE1 provides the range in between two water bodies (B and C) while the Range-Chronogram shows the hyperbolic signatures of these two water bodies. The situation is worse in the vicinity of water bodies C, D, E.

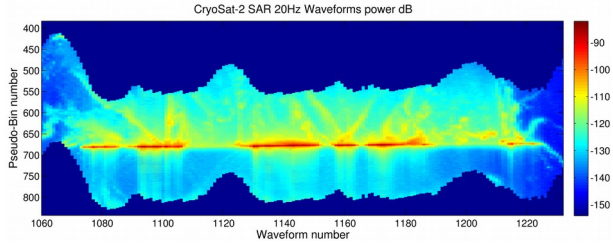

Figure 2. CryoSat-2 SAR 20Hz waveforms Range-Chronogram over multiple water areas in the Amazon. Data kindly provided by Salvatore Dinardo, Nov. 2012 (ESA).

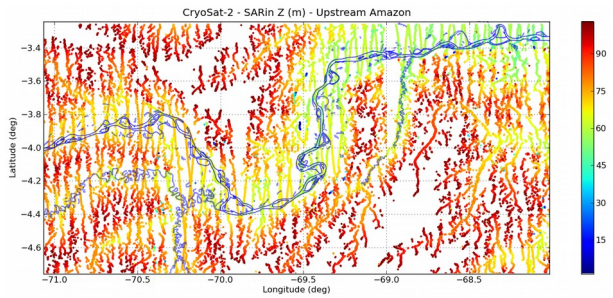

Figure 3. CryoSat-2 ESA/L2 SARIn products upstream Amazon. The “loss” of the ground tracks pattern confirms that the altimeter is sensitive enough to very off-nadir water targets.

The inland water scenarios is not only very diverse but also subject to space and time variability. These properties combine with the off-nadir sensitivity of the instrument and result in the loss of accuracy and precision in alti-hydrology measurements. This occurs through land contamination at nadir and multiple off-nadir water contributions. Even repeat orbit altimeters which permit the use of Fixed Virtual Stations (FVS) or Fixed Satellite Gauging Stations (FSGS) are subject to such disturbances.

In this context, how can we use CryoSat-2 data to characterize Sentinel-3 waveforms over inland waters ? And also, how can we derive water heights with a consistent accuracy and precision over time in both SARM and LRM ?

To our point of view the answers to both questions require to abandon the principle of FVS even on repeat track orbits. FVS are manually defined as the intersection area of satellite track and a static pre-defined riverbed, which 1st is too much work to cover the whole globe, 2nd is too sensitive to orbit change or drift (e.g., SARAL mission) and local morphological changes. Maintaining FVS is a hard and manual work such that it restricts data acquisition to the most large rivers, inducing a huge under-sampling of hydrological basins.

The delimitation of Satellite Gauging Stations should be adaptive to the actual inland water "ground truth".

For this reason we set up a new framework that enables the automated exploitation of water masks.

2. A NEW AND FLEXIBLE FRAMEWORK FOR ALTI-HYDROLOGY

In the previous section we established that the proper handling of radar altimeter data goes through the best possible use of a priori information on the water content within the instrument footprint. In this section, we introduce a new framework capable of taking into account a priori information on the water content within the instrument footprint. This framework is also intended to ease the automated interpretation and editing / masking of data at different processing levels toward accurate, precise and consistent water heights and time series.

This new framework is inherently adaptive to the existing water masks. It is also a trampoline to the synergistic inter-operation with radar imaging missions such as Sentinel-1 (and ENVISAT for past LRM missions). Even-though C band radar imagers are lower resolution than optical imagers, their main advantage is to ensure the regular update of water masks thanks to their all-weather and night and day imaging capabilities. ALONG-TRACK S.A.S. initiated in-house works that will soon exploit Sentinel-1 data in order to produce up-to-date water masks [Fabry et al. 2015a]. They will be used in synergy with CryoSat-2 and Sentinel-3 data to :

- improve the characterization of L1B data products and possibly backward analyse L1A and L1B-S data products,
- improve water height measurements selection at the output of the existing retrackers output even though they are not designed for the inland water domain.

2.1. Principles

Beam-Doppler limited footprint are computed, at each record, from the useful parameters (longitude, latitude, tracker range, satellite altitude and velocity) found in the CryoSat-2 L1B product files and the system parameters (3dB antenna beam-width, burst PRF). As depicted in Figure 4 (and zoomed in Figure 5), the Beam-Doppler limited footprints are superimposed with the water masks in the local Earth-tangential plane (ENU: East North-Up). This makes it possible to compute, for each footprint, the total number of pixels (NP) as well as the number of water pixels (NWP) at the intersection with the water masks. We then define the **fraction of water pixels** (FWP) as FWP = NWP / NP.

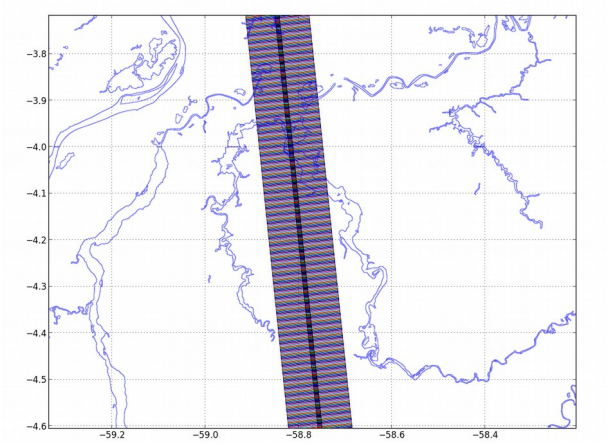

Figure 4. SRTM/SWBD water masks (tiles: w059s04s, w059s05s, w060s04s, w060s05s) superimposed with the series of CryoSat-2 Beam-Doppler limited footprints (20Hz records) generated over small tributaries of the Madeira and Amazon rivers. Baseline B, SAR L1B data on 2014-04-16-T090624.

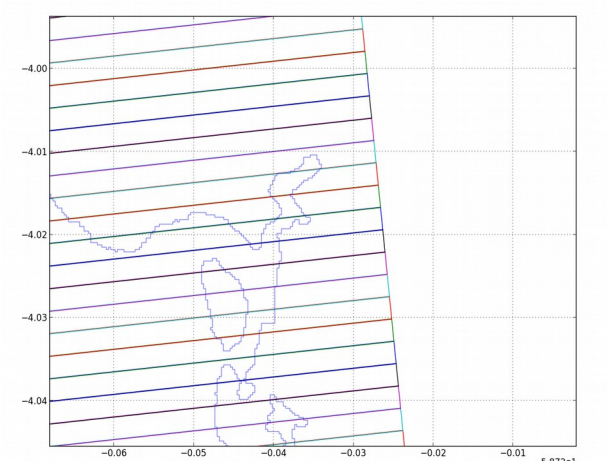

Figure 5. Zoom on the upper central part of Figure 4.

2.2. Details of the Footprints generation

The along-track or Doppler limited footprint size, illustrated in Figure 6, is related to the satellite velocityV_{sat}, central wavelength λ, its range to ground h and the burst PRF:

$$\Delta x = h.\frac{\lambda}{2V_{sat}}.\frac{PRF}{64}$$

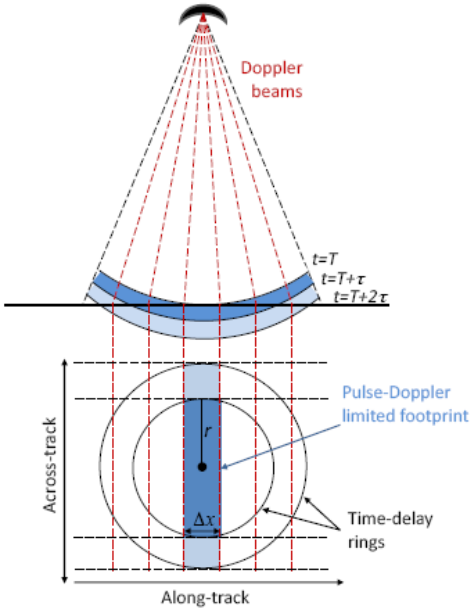

Figure 6. Illustration of the along-track or Doppler limited footprint size, taken from the [CryoSat-2 Handbook, 2013].

A reasonable approximation of the across-track beam size D is:

$$D = h.\tan(\theta_B + \frac{\upsilon}{2}) - h.\tan(\theta_B - \frac{\upsilon}{2})$$

where,

- θ_B is the 3dB across-track antenna aperture (1.2 deg),
- υ is the boresight angle w.r.t. nadir (0 deg in this study but it can be computed from the attitude angles and several rotations in the satellite centred reference frame).

Both Δx and D are computed at each record's location with the updated parameters and the pixel numbers N and NW as well as the water fraction FWP are derived from the intersection with the water mask.

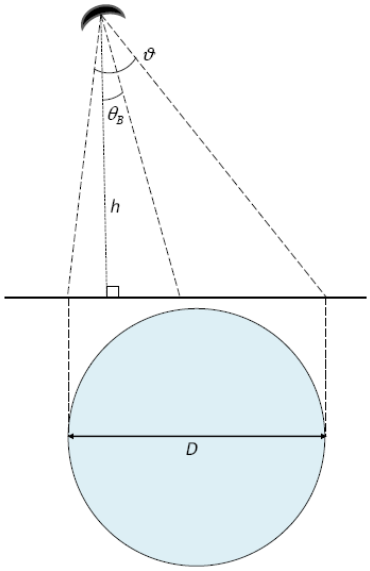

Figure 7. Illustration of the beam limited footprint size, taken from the [CryoSat-2 Handbook, 2013].

2.3. Use of the framework for SARM data characterization

We now use the new framework to check whether the Range Integrated Power Distributions[1] (RIP) have remarkable properties as a function of the FWP, or not.

While reading the acquisition parameters for each record and building the Beam-Doppler limited footprints we also access the beam behaviour parameters contained in the L1B products. The following parameters are derived from the fit of the RIP with a Gaussian PDF :

– Stack Scaled : amplitude normalised to 65535 which can be converted to a power in Watts,
– Mean Centre of the Gaussian PDF fitting the RIP,
– Stack Standard Deviation of the Gaussian PDF fitting the RIP,
– Stack Skewness : asymmetry of the RIP,
– Stack Kurtosis : peakiness of the RIP.

1 RIP. is a 1D signal resulting from the range-wise summation of the 2D Multi-Look Stack (1 stack per record), while the sum in the along-track direction provides the 20Hz SAR waveform.

3. EXPERIMENT

The study period extends from 2014-01-03 to 2014-02-14. We consider a wide area around the confluence of rio Xingu with the Amazon. The water masks covering this area are in the following SWBD tiles: 'w052s02s', 'w052s03s', 'w053s02s' and 'w053s03s'. The following CryoSat-2 Baseline B, L1B, SARM files are used:

CS_OFFL_SIR_SAR_1B_20140103T134052_20140103T134306_B001.DBL
CS_OFFL_SIR_SAR_1B_20140105T133827_20140105T134040_B001.DBL
CS_OFFL_SIR_SAR_1B_20140107T133601_20140107T133814_B001.DBL
CS_OFFL_SIR_SAR_1B_20140117T010011_20140117T010225_B001.DBL
CS_OFFL_SIR_SAR_1B_20140119T005745_20140119T005959_B001.DBL
CS_OFFL_SIR_SAR_1B_20140121T005519_20140121T005732_B001.DBL
CS_OFFL_SIR_SAR_1B_20140130T121823_20140130T122037_B001.DBL
CS_OFFL_SIR_SAR_1B_20140201T121556_20140201T121811_B001.DBL
CS_OFFL_SIR_SAR_1B_20140203T121330_20140203T121544_B001.DBL
CS_OFFL_SIR_SAR_1B_20140205T121104_20140205T121318_B001.DBL
CS_OFFL_SIR_SAR_1B_20140212T233737_20140212T233950_B001.DBL
CS_OFFL_SIR_SAR_1B_20140214T233510_20140214T233724_B001.DBL.

4. RESULTS

When analysing the results it is important to consider that, in this experiment, we keep all of the records which Beam-Doppler footprint is entirely inside the tiles of interest. The histogram in Figure 8 illustrates the natural land cover distribution of non-water (FWP=0) and water (FWP>0) surfaces where low FWP classes are over-populated compared to the others. This distribution is also biased by (1) limitations inherent to the design of the SWBD water masks from which water surfaces under a given threshold are discarded [SRTM, 2003] and (2) possible surface classification errors in SWBD tiles. Also, in order to compare classes with similar populations we should process more files and randomly reject some members in the over-populated classes.

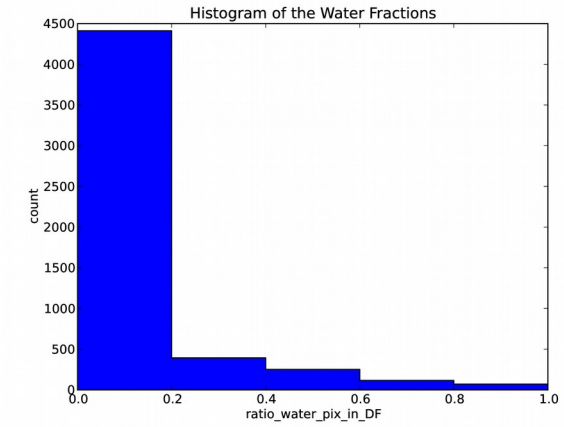

Figure 8. Histogram of the Fraction of Water Pixels found in the Beam-Doppler footprints of the processed CryoSat-2, L1B, SARM data.

Despite the unbalanced populations, it seems that the backscattered energy in classes with a high FWP is better defined and consistent than those with low FWP. This trend appears in Figure 9 where the scaled amplitude of the RIP is plotted versus the FWP.

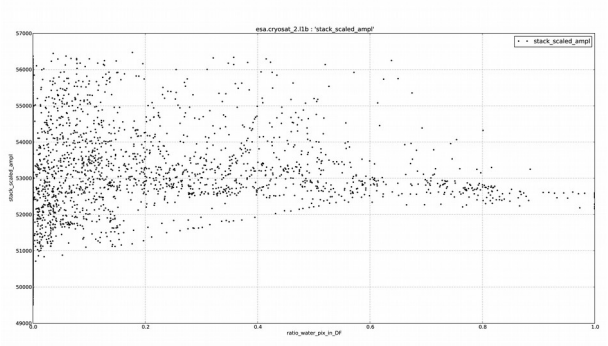

Figure 9. Scaled amplitude of the RIP versus the Fraction of Water Pixels in the Beam-Doppler footprints.

A thorough analysis of the outliers in the intermediate classes (classes with FWP ranging from about 40% to about 80%) could help confirm this reasonable property of backscattering surfaces. Nevertheless it is clear that these intermediate classes, each with actually a significant amount of water, host cases ranging from “most of the water area is at nadir” to “most of the water area is at far end” of the footprint. It can be expected that, for a given water fraction, the footprint power contribution into the Doppler beams (or angular response in the RIP) depends on the across-track distribution of the water surface.

The Standard Deviation of the RIP is an indication on how the energy is backscattered from the surface within the footprint into the many Doppler Beams (azimuth look angles). Figure 10 shows that footprints with a very small water content tend to have a smaller RIP Standard Deviation which could mean that they are sensitive to bright targets (possibly because of small water surfaces not accounted for in SWBD water masks). On the opposite footprints which are all over water (FWP>80%) do have a larger RIP Standard deviation because their footprints exhibit strong backscatter properties in all directions (in all looks).

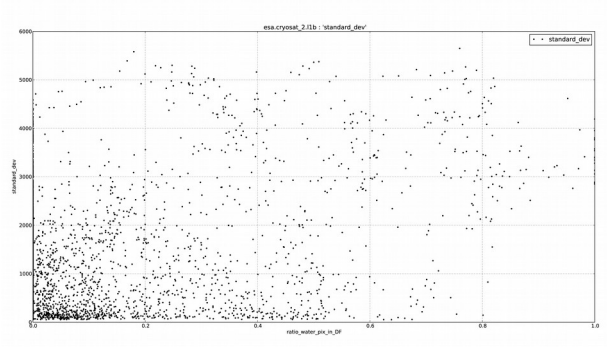

Figure 10. Standard Deviation of the Gaussian PDF fitting the RIP versus the Fraction of Water Pixels in the Beam-Doppler footprints.

The Stack Centres in Figure 11 seem to vary more for the very low FWP (<15%) than for the others, which confirms the diversity of this class and the sensitivity to bright targets (water or habitations). For these lower FWP values, Stack Centres point clouds depict horizontal structures that seem related to either (a) surfaces of various along-track mean slope and/or to (b) platform mispointing in the across-track direction, (c) side lobe effects in the along-track direction. This point will be addressed in future work. Unfortunately no other trend can be identified for the remaining water fractions.

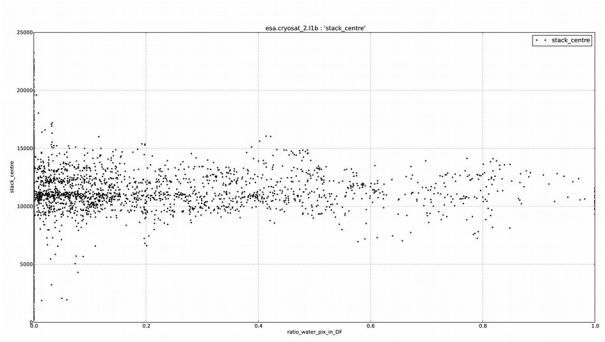

Figure 11. Stack Centre versus the Fraction of Water Pixels in the Beam-Doppler footprints.

In practice the actual power of the looks (and therefore the shape of the RIP) is impacted by several contributions:

- the water fraction (FWP),
- the distribution of WP across the Doppler Footprint, weighted by range-gate surface areas (thus the across track distribution of water may affect the footprint response vs look angles),
- the along-track evolution of the FWP combined to the antenna side lobes. The looks for which a side lobe is directed to a water area will have a ghost contribution to the RIP, thus modifying the shape of the RIP and the fitted parameters.

In the objective of assessing the potential of water detection from SARM altimetry, we checked the potential relation between several of the RIP fitted parameter. Figure 12 and 13 show that a RIP with high Standard Deviation correspond to low Kurtosis values (very wide angular response of footprints that have a high water content or high FWP). For the lower Standard Deviation the situation is more complicated w.r.t. FWP. Nevertheless it can seems that The Kurtosis or peakiness tends to evolve inversely to the Standard Deviation.

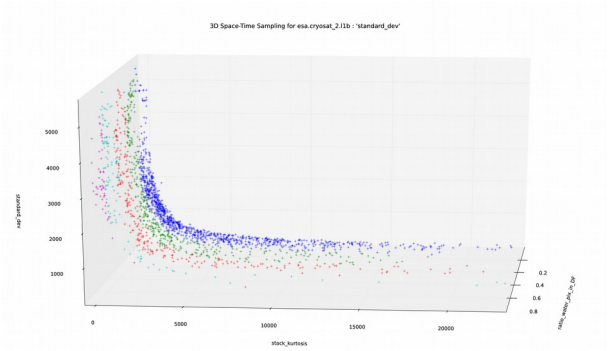

Figure 12. Standard Deviation of the Gaussian PDF fitting the RIP versus the Kurtosis of the RIP and Fraction of Water Pixels in the Beam-Doppler footprints. FWP are separated with into 5 coloured classes 20% wide.

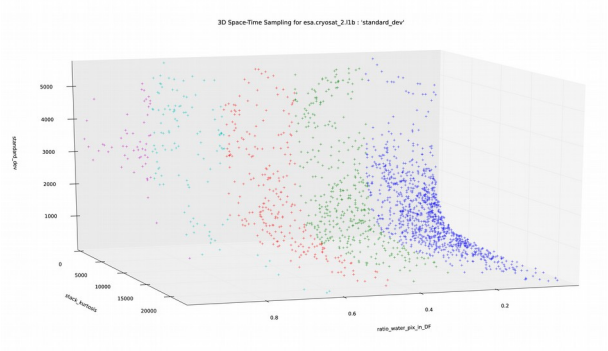

Figure 13. same as figure 12 from another view point.

On the other hand Figures 14 and 15 show a non water-discriminant relationship between Stack skewness and both the Kurtosis and the FWP.

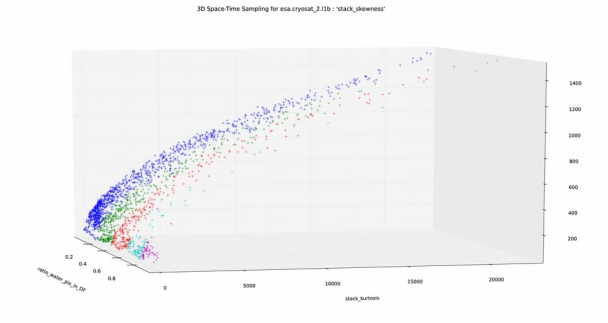

Figure 14. Skewness of the RIP versus the Kurtosis of the RIP and Fraction of Water Pixels in the Beam-Doppler footprints. FWP are separated with into 5 coloured classes 20% wide.

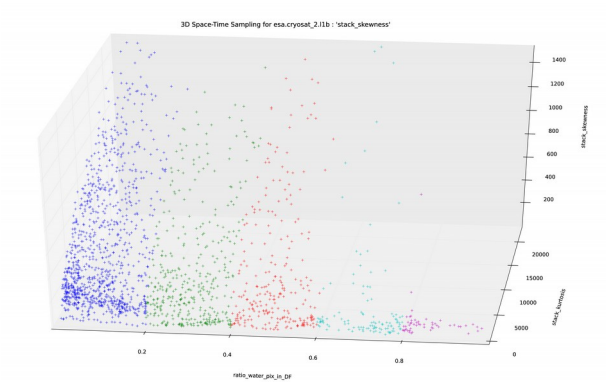

Figure 15. same as figure 14 from another view point.

5. CONCLUSIONS

Our main objective in this study was to establish a new framework and to have a quick check whether the Range Integrated Power parameters would have remarkable features versus the FWP. These very preliminary results are difficult to interpret since many issues are entangled together :

1. We probably did not process enough data and, as shown in the histogram, high water fraction footprints are poorly represented. We absolutely need to process more data and reject the footprints that are too far away from the water mask,
2. The intermediate classes (i.e., with theoretical water content ranging from about 40% to about 80%) are in fact too diverse since they host cases ranging from “most of the water area is at nadir” to “most of the water area is at far end” of the footprint.
3. The water masks used here are very old (2003) and probably not adequately resolved and not exhaustive enough regarding smaller water surfaces [SWBD, 2003]. The classes that we define as low FWP classes from these water masks may in fact contain wet areas with flooded forests (and the altimeter may sense them),
4. The results may be specific to this part of the Amazon basin.
5. The WP are not weighted with respect to their relative position into the Doppler-Footprints.

Nevertheless, it seems that
- The backscattered energy in classes with a high FWP is better defined and consistent than those with low FWP.
- Footprints with a very small water content tend have a small RIP Standard Deviation which could mean that they are sensitive to bright targets (possibly water not accounted for in water masks). On the opposite footprints which are all over water do have a larger RIP Standard deviation because the footprint exhibit strong backscatter properties in all directions (in all looks).

6. ONGOING WORK AND PERSPECTIVES

We are currently working on two major improvements of the new framework . The first one is to introduce the Pulse-Doppler limited footprint so as to discriminate whether the water pixels are at nadir or not (we introduce the FWPN : Fraction of Water Pixels at NADIR). We also are working on the weighting of the water pixels according to their distance to nadir

7. BIBLIOGRAPHY

Bercher N., Calmant S. Fleury S., Dinardo S., Boy F., Picot N. et Benveniste, J. (2014a). “CryoSat-2 over rivers: a present mission, an insight into the future of altimetry”. In Proceedings of the OST/ST, 27-31 October, Lake Constance, Germany. Oral communication.

Fabry, P. and Bercher, N. (2015a). “A step Toward the Automated Production of Water Masks from Sentinel-1 images”, Mapping Water Body from Space Conference, 18-19 March 2015. ESRIN, Frascati. Oral communication.

ESA-UCL, CryoSat-2 Product Handbook, April 2013.

SRTM Water Body Data Product Specific Guidance (v.2.0, March 12, 2003), http://dds.cr.usgs.gov/srtm/version2_1/SWBD/SWBD_Documentation/, NASA/NGA.